IEEE Access
Multidisciplinary | Rapid Review | Open Access Journal

Received 29 November 2023, accepted 8 January 2024, date of publication 10 January 2024,
date of current version 19 January 2024.

*Digital Object Identifier 10.1109/ACCESS.2024.3352546*

RESEARCH ARTICLE

# Output Regulation-Based Optimal Control System for Maximum Power Extraction of a Machine-Side Power Converter in Variable-Speed WECS

**BAYANDY SARSEMBAYEV[1,2], NURKHAT ZHAKIYEV[1,3,4], ALMAN KUSHEKKALIYEV[3], KORHAN KAYISLI[4], (Senior Member, IEEE), AND TON DUC DO[5], (Senior Member, IEEE)**

[1]Department of Science and Innovation, Astana IT University, Astana 010000, Kazakhstan
[2]Department of Aerospace and Environment Engineering, School of Engineering and Digital Sciences (SEDS), Nazarbayev University, Astana 010000, Kazakhstan
[3]Department of Physics, West Kazakhstan University, Uralsk 090000, Kazakhstan
[4]Department of Electrical-Electronic Engineering, Engineering Faculty, Gazi University, 06560 Ankara, Turkey
[5]Department of Robotics and Mechatronics, School of Engineering and Digital Sciences (SEDS), Nazarbayev University, Astana 010000, Kazakhstan

Corresponding author: Korhan Kayisli (korhankayisli@gmail.com)

This work was supported by the Ministry of Science and Higher Education, Kazakhstan, under Grant AP09261258. The work of Nurkhat Zhakiyev and Korhan Kayisli was supported by the Scholarship Programme from the Islamic Development Bank under Grant 2021-588606.

**ABSTRACT** In this study, the integral linear quadratic regulator (LQR) with servomechanism for machine-side power converter in PMSG-based variable-speed wind energy conversion systems (WECSs) has been proposed. The solution of the algebraic Riccati equation (ARE) has been found for the extended dimension of the state space equation of the system. The state vector has been extended with the integral of the angular shaft speed of the permanent magnet synchronous generator (PMSG) to penalize the errors. The maximum power tracking point (MPPT) algorithm is achieved by minimizing tracking errors between the angular shaft speed reference based on wind speed estimation and its actual values in the variable speed WECS. Also, the estimated aerodynamic torque is used to define the reference electromagnetic torque. This is possible when WECS is partially loaded and pitches angles are fixed at the position to generate maximum power. The mean absolute percentage error of the angular shaft speed of the PMSG-based WECS has been reduced by more than 71% under model uncertainty and noise presented case than in the traditional disturbance observers-based compensation scheme. While the disturbance observers for estimation model uncertainty are eliminated, the use of the high order disturbance observer for aerodynamic torque estimation proved to be necessary to enhance the reliability of wind speed sensors and hence the whole WECS.

**INDEX TERMS** Wind energy conversion system (WECS), permanent magnet synchronous generator (PMSG), linear output feedback controller, integral servomechanism-based control, linear quadratic regulator (LQR), optimal tip speed ratio (TCR), maximum power point tracking (MPPT).

## I. INTRODUCTION

Wind power has the growing potential to be converted from rotating mechanical energy into electricity. Wind energy conversion systems (WECSs) have great potential for growth in electric power generation among other renewable energy sources in Kazakhstan. The directly connected variable-speed WECS configuration can produce more power whereas the pitch angles of the blades are fixed at zero degrees. However, the control system's performance of the machine-side power converter can deteriorate due to model uncertainty in PMSG, modeling errors in WECS, and external disturbance caused by wind speed variation [1], [2], [3]. The external disturbances in WECS are associated with wind speed, viscous frictions, and other mechanical factors whereas model uncertainty is associated with mechanical and electrical parameter

The associate editor coordinating the review of this manuscript and approving it for publication was Laura Celentano.

variations. In real-time applications, unmodelled dynamics are associated with noise and offsets from the measuring apparatus such as current and voltage sensors, position encoders, torques transducer, as well as generator's body structure induced torque, dead-time effects in the power converters. The design of a control system for a machine–side converter with the ability to facilitate minimum angular shaft speed tracking error under disturbance effects for maximizing power extraction in WECS is an important task.

The tip-speed ratio (TCR), perturbation and observation (P&O), and optimal relationship-based (ORB) approaches are mainly used to extract maximum power in WECS applications. While in the P&O-based maximum power point tracking (MPPT) algorithm, the golden section search method or hill climbing search methods can be used for perturbation and measurement of the generator's speed for search peak output power [4], the ORB-based MPPT algorithm is operated with optimum relations between the different system parameters pre-calculated in advanced and stored in the look-up tables [6]. The TCR-based MPPT is based on prior acquired wind speed information and has a comparatively fast response whereas the straightforward method is to achieve optimal output power with partially loaded WECS [7]. The MPPT control algorithm relies on the accurate measurement of the effective wind speed blowing to the blades of the WECSs. However, these measurements are disturbed by turbulent wind induced by the turbine's blades. Moreover, the wind sensors might have faults, which also adds to the cost of the overall system. While the wind speed can be measured with cap anemometers, it also can be estimated via linear and nonlinear disturbance observers (DOs) with the Newton-Raphson search method solved numerically. The perturb and observe (PO) is another method with a hill climbing search algorithm that does not require a plant model. The nonlinear Tagaki-Sugeno observer is another approach proposed to estimate wind speed to guarantee improved performance and robustness in the presence of uncertainties [8]. This observer is based on a reduced-order model of the WECS.

The proportional-integral (PI) controllers-based WECSs are straightforward due to the simplicity of the algorithms but are sensitive to parameter variations and disturbances. This requires tuning the PI gains again or designing adaptive gains under certain conditions. In this regard, many control approaches are developed to compensate for disturbances in the WECS in feedforward and feedback schemes. The disturbance observer-based controls (DOBCs) use sophisticated disturbance observers such as sliding mode observer (SMO) [9], high-order disturbance observer (HODO) [10], [11], [12], [13], extended state observer (ESO) [14], [15], [16], [17], in feedforward scheme along with base feedback controller. While HODO synthesized with linear [12], [18], [19], and nonlinear [10], [11], [20], feedback controllers are associated with DOBC, the ESO synthesized with feedback controllers are called active disturbance rejection control (ADRC) [14], [15], [16], [21] which has shown its superiority over field-oriented (FOC) approach [17]. These approaches compensate for the disturbances in the feedforward scheme with model-based baseline controllers, others suppress the lumped disturbances with pre-trained or online intelligent feedback controllers only [9], [21], [22], [23], [24], [25].

The DOBC technique is one way to reduce the impact of disturbances and model uncertainty on the performance of WECS. The linear and nonlinear feedback control systems are synthesized with high-order disturbance observers (HODOs) where the uncertainties are compensated via feedforward parts of the proposed schemes. While the external disturbance and model uncertainty are estimated with nonlinear HODOs, the feedback control parts' approaches have been improved to suppress the disturbances in these studies [12], [18]. Particularly, the ISMC with a linear feedback controller as a nominal part has been proposed to reduce tracking errors and hence maximize power extraction in the WECS [10], [11]. The state-dependent Riccati equation (SDRE) based ISMC to account for the nonlinear multivariable structure of the system has been proposed in the study. The large gain selection, for ensuring the reaching sliding mode amplifies the chattering inherited from traditional SMC, the integral sliding mode control (ISMC) method can be used to eliminate the reaching mode in the sliding variable. The integral-based sliding variables have eliminated the reaching phase and chattering has been reduced significantly with continuous approximation in the switching function of the control law. In these control systems, the external disturbance and model uncertainty have been estimated via HODOs. While HODO assumes the aerodynamic torque and uncertainties are smooth enough for estimations, the requirement for slow-varying disturbance assumption has been removed [12]. Moreover, the sensorless approach with HODO for the estimation of aerodynamic torque eliminates reliance on the wind sensors.

While the extracted power generated by WECS can be impacted by disturbance, the quality of power flowing between it and the grid also can be affected. The extended state observer (ESO) is the core of the ADRC approach for estimating lumped disturbances. The multi-loop ADRC scheme with ESOs has been proposed to regulate flows of active and reactive power in the speed and current loops [2]. Later they updated the design with the two-degree-of-freedom internal model controller (TDFIMC) approach to improve the quality of the power [14]. The set-point and filter parameters are regulated to improve the active and reactive power generated by the WECS. The model-assisted sensorless ADRC with a nonlinear Kalman filter for estimation of the angular speed has been proposed to improve the tracking performance of the WECS [21]. The IC technique intends to enhance MPPT control due to changes in the initial characteristics of WECS which can be degraded over time or under operational conditions. The Q-learning method-based reinforcement learning (RL) algorithm has

been proposed to train artificial neural networks (ANN) online [26]. Once the controller is trained with RL, it can switch to optimal relationship-based MPPT control. However, these methods are complicated and their algorithms require following complex mathematical rigor. Moreover, the online control methods based on ANN require large memory for computations and a long training procedure with data before the use of the controller [26].

Recently, the linear output regulation method with a servomechanism-based technique has been applied to the missile autopilot system to improve its tracking performance [27]. Particularly, the servomechanism-based state-dependent Riccati equation (SDRE) control approximated with Taylor series expansion has been proposed to account for nonlinearities in the internal dynamics of the PMSG. In the control design, the multivariable nonlinear structure is captured with the SDRE method transforming it into pointwise linear dynamics [28]. While servomechanism has been incorporated into the SDRE approach, it has not been thoroughly tested with a linear quadratic regulator (LQR). Moreover, the study has demonstrated a slight improvement in tracking performance. Therefore, a comprehensive analysis of the closed-loop stability is also aimed in this study.

In this study, a servomechanism-based optimal controller with linear output feedback is proposed to maximize power extraction in the variable speed WECS under nominal parameters and parameter perturbations. Unlike to conventional approach to estimating uncertainties with disturbance observers, the lumped disturbances are suppressed with the proposed servomechanism-based linear feedback control regardless of the presented nonlinear multivariable structure of the system and model uncertainty. The optimal gain matrix for augmented state space equations is obtained by solving offline the linear quadratic regulator (LQR) problem as in the conventional one. The HODO observer is utilized for wind speed estimation to enhance the reliability of the whole system. It is assumed the DC-link voltage is assumed to be fixed to assess the efficiency of the proposed control system for the machine-side converter.

The paper is organized as follows: the second section will detail the PMSG-based WECS model, followed by the control system design and its stability analysis. The comparative simulation results of the proposed control system will be presented in the third section. Finally, concluding remarks will be provided in the fourth section.

## II. WIND ENERGY CONVERSION SYSTEM

### A. WIND TURBINE MODELING

The back-to-back (B2B) power converter is usually used to regulate the power flow between a WECS and grid [29]. The machine-side power converter of the back-to-back (B2B) converter is depicted in Figure 1. The full-rated B2B power converter is separated by two converters with a DC-link capacitor. by two, namely and grid-side converters.24 While the machine-side converter is responsible for extracting

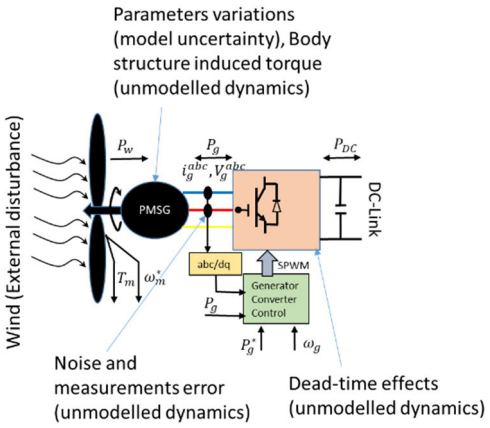


**FIGURE 1.** Machine-side part of the back-to-back power converter for WECS.

maximum power from wind power, the grid-side converter feeds this power to the connected grid at stable constant power and synchronous frequency.

The available aerodynamic power is a function of power coefficient, $C_p(\lambda, \beta)$, WT's dimensions (rotor radius), air density, $\rho$, and cubic wind speed,

$$P_a = \frac{1}{2}\rho\pi R^2 C_p\left(\lambda, \beta\right) v^3 \tag{1}$$

The power coefficient depends on the tip speed ratio (TCR), $\lambda$, and pitch angles of the blades, $\beta$ if they are controllable.

The wind turbine (WT) can operate at partial load and full load modes. While at partial load pitch angles can be set at zero degrees to facilitate less resistance from the blades, the pitch angles can be regulated such that they resist air flowing to limit the rotating speed of the shaft hence limiting overrated power extraction $\beta$ [30].

*Assumption 1:* The given WECS is operated under partial load mode, therefore pitch angles are not regulated to limit power.

The TCR directly relates to WT's angular shaft speed, $\omega_t$ and versa proportional to wind speed [11]

$$\lambda = \frac{\omega_t R}{v} \tag{2}$$

The rotating speed of the shaft of the WT is a function of optimal TSR, $\lambda_{opt}$ unless it corresponds to the upper or lower rotating speed limits of WT. Therefore, its form operated in partial load with fixed blades' pitches angles will be following [12]

$$\omega_{t,d} = \frac{\lambda_{opt} v}{R} \tag{3}$$

Similar to the aerodynamic power, the aerodynamic torque is the function of quadratic wind speed and torque coefficient [13]

$$T_a = \frac{P_a}{\omega_t} = \frac{1}{2}\rho\pi R^3 C_q\left(\lambda, \beta\right) v^2 \tag{4}$$

where $C_q\left(\lambda, \beta\right) = C_p\left(\lambda, \beta\right)/\lambda$ is the torque coefficient.

### B. PMSG MODEL IN A D-Q REFERENCE FRAME

Let's consider the dynamic system's equations of the PMSG in the WECS in the d-q reference frame where electromagnetic torque is the function of quadrature current [28],

$$\begin{cases} \dfrac{d\omega}{dt} = \dfrac{1}{Jn_{gb}}T_a - \dfrac{B}{J}\omega - \dfrac{1}{J}T_e \\ \dfrac{dT_e}{dt} = -PK\omega i_d - \dfrac{R_s}{L}T_e - \dfrac{\psi_m PK}{L}\omega + \dfrac{K}{L}V_q + d_q \\ \dfrac{di_d}{dt} = \dfrac{1}{L}V_d - \dfrac{R_s}{L}i_d + \dfrac{P}{K}\omega T_e + d_d \end{cases} \tag{5}$$

where $\omega$ is the angular shaft speed of PMSG, $i_d$ is the d-axis stator current, and $V_d$ and $V_q$ present the stator voltages on the d-axis and q-axis, respectively; $R_s$ is stator resistance; $L$ is stator inductance; $B$ is viscous friction coefficient; $\psi_m$ denotes magnetic flux linkage; $J$ presents rotor inertia; $P$ is pole pairs, and $T_e$ is electromagnetic torque.

$$T_e = Ki_q \tag{6}$$

where, $K = 3/2(\psi_m P)$.

The d-q disturbances presented in the system are [11],

$$d_q = \left(\frac{R_s}{L} - \frac{R_s + \Delta R_s}{L + \Delta L}\right) T_e + \left(\frac{1}{L} - \frac{1}{L + \Delta L}\right) \psi_m PK\omega + \left(\frac{1}{L} - \frac{1}{L + \Delta L}\right) KV_q + d_{qn} \tag{7}$$

$$d_d = \left(\frac{R_s}{L} - \frac{R_s + \Delta R_s}{L + \Delta L}\right) i_d + \left(\frac{1}{L} - \frac{1}{L + \Delta L}\right) V_d + d_{dn} \tag{8}$$

where $\Delta R_s$ and $\Delta L_s$ are uncertainties due to electrical parameter variations of the PMSG, and $d_{qn}$ and $d_{dn}$ are the noise associated with sensor accuracy and modeling errors from hardware apparatus.

### C. CONTROL SYSTEM DESIGN

In this section, the conventional LQR-based feedback control will be transformed into the proposed servomechanism-based linear feedback control law. To facilitate the optimal work of the variable speed WECS via the MPPT algorithm, the HODO structure with its main features will be presented as well.

#### 1) SERVOMECHANISM-BASED LINEAR FEEDBACK CONTROL LAW DESIGN

Let's take the performance index of the linear quadratic regulator problem for its minimizing with input $u$ [11].

$$\text{Min } J(u) = \frac{1}{2}\int_0^\infty x^T Qx + u^T Rudt \tag{9}$$

where $Q$ and $R$ are semi-definite state and control input weighting matrices, $Q \geq 0$ and $R > 0$ with corresponding dimensions to the state variables of $x$

Let's take a time-invariant linear state space model of the system

$$\dot{\tilde{x}} = \bar{A}\tilde{x} + \bar{B}u. \tag{10}$$

The state-space model of the system has to be extended by the penalty state, and the partition of the extended state and control matrices will be presented as follows, [28]

$$\bar{A} = \begin{bmatrix} 0 & I \\ A & 0 \end{bmatrix}, \bar{B} = \begin{bmatrix} 0 \\ B \end{bmatrix} \tag{11}$$

The error of each state variable can be found as

$$\tilde{\omega} = \omega - \omega_d, \omega_d = \omega_{t,d} \cdot n_{gb} = \frac{\lambda_{opt}}{R}\vartheta \cdot n_{gb},$$
$$\tilde{T}_e = T_e - T_{ed}, T_{ed} = \frac{1}{n_{gb}}T_a - B\omega_d - J\dot{\omega}_d \tag{12}$$

The state vector is formed as $\tilde{x}^T = \begin{bmatrix} \int \tilde{\omega}dt & \tilde{\omega} & \tilde{T}_e & i_{ds} \end{bmatrix}$, and the control vector is $u^T = \begin{bmatrix} V_q V_d \end{bmatrix} = \begin{bmatrix} u_{fbq} u_{fbd} \end{bmatrix}$.

Considering the state variables defined in equation (12) with the integral of error of angular shaft speed acting as a penalty function, the generator's dynamics will be as follows,

$$\begin{cases} \int \tilde{\omega}dt = 0 \\ \dfrac{d\tilde{\omega}}{dt} = -\dfrac{B}{J}\tilde{\omega} - \dfrac{1}{J}\tilde{T}_e \\ \dfrac{d\tilde{T}_e}{dt} = -PL\tilde{\omega}i_d - \dfrac{R_s}{L}\tilde{T}_e - \dfrac{\psi_m PK}{L}\tilde{\omega} + \dfrac{K}{L}V_q \\ \dfrac{di_{ds}}{dt} = \dfrac{1}{L}V_d - \dfrac{R_s}{L}i_d + \dfrac{PL}{K}\tilde{\omega}\tilde{T}_e \end{cases} \tag{13}$$

The extended states and control matrices are

$$\bar{A} = \begin{bmatrix} 0 & 1 & 0 & 0 \\ 0 & -\frac{B}{J} & -\frac{1}{J} & 0 \\ 0 & -\frac{\psi_m PK}{L} & -\frac{R_s}{L} & 0 \\ 0 & 0 & 0 & -\frac{R_s}{L} \end{bmatrix}, \bar{B} = \begin{bmatrix} 0 & 0 \\ 0 & 0 \\ \frac{K}{L} & 0 \\ 0 & \frac{1}{L} \end{bmatrix} \tag{14}$$

Let's define the ARE LQ problem as

$$\bar{A}^T\bar{P} + \bar{P}\bar{A} - \bar{P}\bar{B}R^{-1}\bar{B}^T\bar{P} + Q = 0 \tag{15}$$

where $\bar{P}$ is the positive definite matrix, the solution of ARE which drives the cost function (9) to a minimum.

The optimal control gain matrix is

$$u = -R^{-1}\bar{B}^T\bar{P}\tilde{x} = -\bar{K}\tilde{x} \tag{16}$$

The algorithm of implementation of the proposed servomechanism-based linear feedback control for maximizing power extraction by machine-side power converter in the WECS under presence of the external and internal disturbances is presented in Figure 2.

In the proposed servomechanism-based LQR problem, the controller gains are determined by solving the extended ARE associated with the optimal control problem. The solution to this equation yields the feedback gains or the control gains that are used to compute the control law for the system.The controller gains in this problem are selected to minimize a quadratic cost function, which includes the weighted sum of the state and control input quadratic terms. The state weighting matrix includes an additional dimension for the integral of the error angular shaft speed which is typically the unity factor.

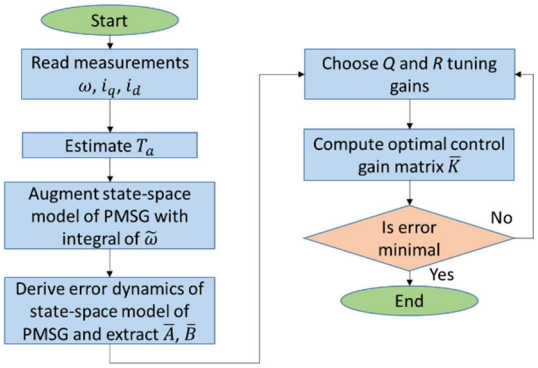


**FIGURE 2.** The algorithm of implementation of the proposed servomechanism-based LQR.

#### 2) STABILITY ANALYSIS

The state vector $\tilde{x}^T = \left[ \int \tilde{\omega} dt \;\; \tilde{\omega} \;\; \tilde{T}_e \;\; i_{ds} \right]$ of the system under the proposed control would converge exponentially to the origin.

Let's take Lyapunov function [11]

$$V(\tilde{x}) = \tilde{x}^T \bar{P} \tilde{x} \tag{17}$$

By combining the equations (10) and (18), it can be shown that the time-derivative of $V(\tilde{x})$ is positive-definite,

$$\begin{aligned} \dot{V}(\tilde{x}) &= \frac{d}{dt}\tilde{x}^T \bar{P}\tilde{x} = 2\tilde{x}^T \bar{P}\left(\bar{A} + \bar{B}\bar{K}\right)\tilde{x} \\ &= 2\tilde{x}^T \bar{P}\left(\bar{A} - \bar{B}R^{-1}\bar{B}^T\bar{P}\right) \\ &= \tilde{x}^T \bar{P}\left(\bar{A}^T\bar{P} + \bar{P}\bar{A} - 2\bar{P}\bar{B}R^{-1}\bar{B}^T\bar{P}\right)\tilde{x} \leq -\bar{x}^T Q\bar{x} \end{aligned} \tag{18}$$

The inequality (18) demonstrates that time derivatives of $V(\tilde{x})$ are negative, therefore, it can be concluded that the value of state vector $\tilde{x}$ converges to the origin exponentially.

### D. AERODYNAMIC TORQUE ESTIMATION

The reliance on wind sensors is eliminated with the use of HODO for estimation of the aerodynamic torque which is proportional to the square of wind speed and coefficient $k_{opt}$ will be obtained. The HODO can estimate fast-varying disturbance unlike to linear disturbance observer which requires the first derivative of disturbance to be zero [31]. In case of a fault in traditional anemometers, this fault-ride-through mechanism enhances the reliability of the whole system.

*Assumption 2:* The assumption is that the aerodynamic torque ($T_a$) is fast-changing but smooth enough to be estimated. The higher than third-order derivatives of $T_a$ could be ignored due to the insignificance impact on the estimation.

To estimate the aerodynamic torque of the WECS angular shaft speed motion equation in (5) is recalled

$$\frac{d\omega}{dt} = \frac{1}{Jn_{gb}}T_a - \frac{B}{J}\omega - \frac{1}{J}T_e \tag{19}$$

**TABLE 1.** The proposed linear feedback control system's parameters.

| Controllers and Observers | Parameters and Gains |
|---|---|
| Controller's gains | Q=diag([1 10000 1000 1]), R=diag([0.0005 0.0005]) |
| Servomechanism type | $\int \tilde{\omega} dt$ |
| Aerodynamic torque, $T_a$ estimator's gains | $L_1$=500, $L_2$=100, $L_3$=20 |

Then, the angular shaft speed-based HODO structure of the aerodynamic torque estimator is

$$\begin{cases} \dot{Z}_\omega = -n_{gb}\left(B\omega + T_e\right) + \hat{T}_a \\ \hat{T}_a = L_{01}g_{01} + L_{11}g_{11} + \ldots + L_{k_1 1}g_{k_1 1} \\ \dot{g}_{01} = Jn_{gb}\omega - Z_\omega \\ \dot{g}_{11} = g_{01} \\ \dot{g}_{21} = g_{11} \\ \vdots \\ g_{k_1 1} = g_{(k_1-1)1}, \end{cases} \tag{20}$$

where $\hat{(\cdot)}$ denotes the estimated variable, and $(\cdot \vdots \cdot)$ is the derivative of the argument functions, respectively, $L_{01}, L_{11}, L_{k_1 1}$ are adjustable gains for the HODO.

Combining (3) and (20) the estimated reference PMSG's rotor speed will be as [10]

$$\hat{\omega}_d = \sqrt{\frac{\hat{T}_a}{k_{opt}}}, \tag{21}$$

where $k_{opt} = \frac{\rho \pi R^5 C_{pmax}}{2\lambda_{opt}^3 n_{gb}^2}$ is the optimal coefficient of TSR under Assumption 1.

## III. SIMULATION RESULTS

In this section, the simulation results of the proposed servomechanism-based linear feedback controller to extract maximum power from wind in small-power WECS are presented. The given WECS parameter are following: rated power $P_{rated} = 5\ kW$; $R_s = 0.3676\ Ohm$; $L = 3.55mH$; $\psi_m = 0.2867 \frac{\text{V·s}}{\text{rad}}$; $J = 7.856 \text{kg·m}^2$; $P = 14$; $B = 0.002 \frac{\text{kg·m}^2}{\text{s}}$; rotor radius, $R = 1.84\ m$; $\rho = 1.25 \frac{kg}{m^3}$. The selected gains for the proposed feedback controller are presented in Table 1. The optimal TCR value, $\lambda_{opt} = 8.1$ with pitch angles of the blades of the WT are fixed at zero degrees to maximize power extraction during its partial load operation, therefore power coefficient, $C_p^{max}$ is obtained as 0.411. The dynamic behavior of wind speed is converted to rotational mechanical energy (Figure 3). The model uncertainty of the generator is associated with the stator's windings' resistance parameters and inductance, $R_s$, and $L$ are increased by 20% and 1% respectively [10], [11], [28]. The noises presented in both control channels associated with sensors are sine functions of time, and high magnitudes, $d_{qn} = 10^5 \sin(t)$ and $d_{dn} = 10^3 \sin(t)$. By solving extended ARE

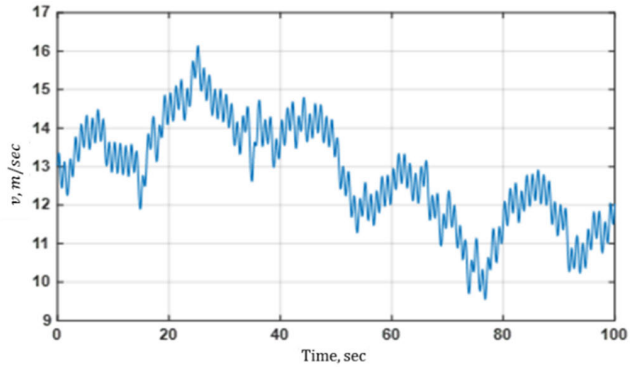


**FIGURE 3.** Wind speed profile with a mean value of 12.13, m/sec [28]. Copyright permission provided.

**TABLE 2.** The servomechanism-based optimal control system's performance.

| Assessment criteria and cases | | Scenario 1 | Scenario 2 | Improved by, % |
|---|---|---|---|---|
| MAPE of angular shaft speed, $\lvert\tilde{\omega}\rvert$ | LQR with compensation [12] | 0.7249 | 0.7246 | - |
| | The proposed control system | 0.2084 | 0.2099 | 71.25%/ 71.03% |
| MAPE of electromagnetic torque, $\lvert\tilde{T}_e\rvert$ | LQR with compensation [12] | 4.9924 | 4.9904 | - |
| | The proposed control system | 5.0075 | 5.0130 | -0.3%/ - 0.45% |
| MAE of d-axis current, $\lvert\tilde{i}_d\rvert$ | LQR with compensation [12] | $4.9267 \times 10^{-5}$ | $4.9251 \times 10^{-5}$ | - |
| | The proposed control system | 0.8532 | 0.8505 | -0.85/- 0.8527 |
| MAPE of aerodynamic torque estimation errors, $\lvert\tilde{T}_a\rvert$ | LQR with compensation [12] | 0.0748 | 0.0735 | - |
| | The proposed control system | 0.0694 | 0.0690 | 7.22%/ 6.12% |

equation (16) with selected state and control input weighting matrices the optimal gains matrix, $\bar{K}$ can be obtained using build-in Matlab's *care* or *lqr* functions. While the gain of the error angular shaft speed is chosen as 10,000, its integral is one. The gain for error of the electromagnetic torque is selected as 1,000, and the direct current gain is one(Table 1). In the diagonal control input weighting matrix, the gains are selected as 0.0005 to reduce steady-state error.

The performance of the proposed servomechanism-based linear feedback control has been compared with conventional LQR control synthesized with the HODOs-based feed-forward compensation technique. The nominal parameters operation and parameters perturbation and noise presented in the system scenarios were assessed to reduce angular shaft speed tracking errors for maximizing power extraction of the variable-speed WECS.

Mainly, the mean absolute percentage error (MAPE) of the generator's angular shaft speed $|\tilde{\omega}|$, MAPE of electromagnetic torque $\left|\tilde{T}_e\right|$, the mean absolute error (MAE) of direct

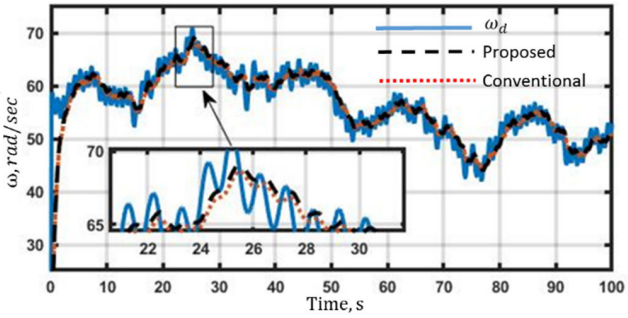


**FIGURE 4.** The presented control and conventional LQR angular shaft speed tracking (scenario 1) [32]. Copyright permission provided.

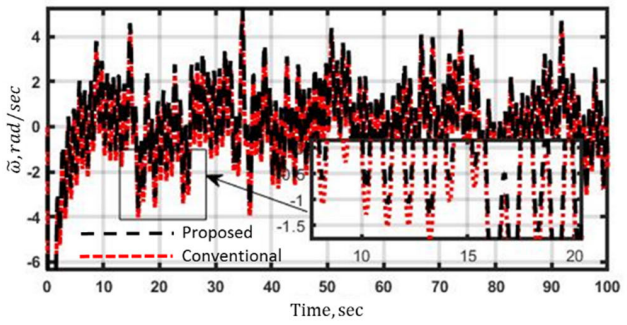


**FIGURE 5.** The presented control and conventional LQR angular shaft speed tracking errors (scenario 1).

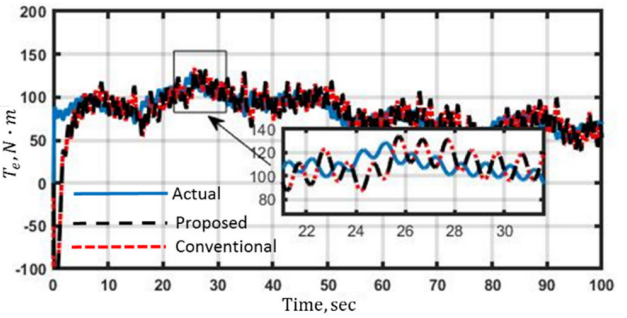


**FIGURE 6.** The presented control and conventional LQR electromagnetic torque tracking (scenario 1) [32]. Copyright permission provided.

axis current $\left|\tilde{i}_d\right|$, and MAPE of the aerodynamic torque estimation $\left|\tilde{T}_a\right|$ have been evaluated (Table 2). The performance of the WECS operation with nominal parameters, scenario 1 depicted in Figures 4-10, and the performance of its operation with parameters perturbation and noise, scenario 2 are presented in Figures 11-17. The disturbance associated with model uncertainty in the quadrature and direct control channels are quantified which are introduced in scenario 2 (Figure 18 and 19).

The MAPE of PMSG's angular shaft speed $|\tilde{\omega}|$ is improved by 71.25% in scenario 1 and by 71.03% in scenario 2 respectively. In both scenarios, the MAPE of aerodynamic torque estimation errors $\left|\tilde{T}_a\right|$ have been reduced by 7.22% and 6.12%

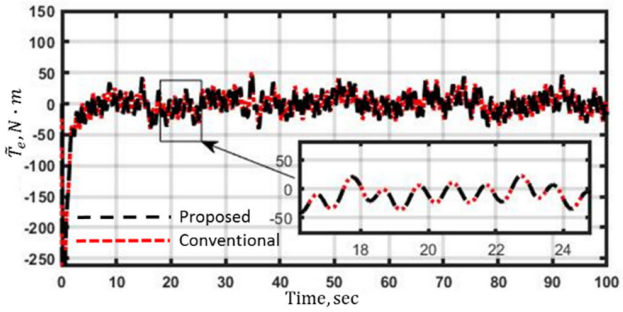


**FIGURE 7.** The presented control and conventional LQR electromagnetic torque tracking errors (scenario 1).

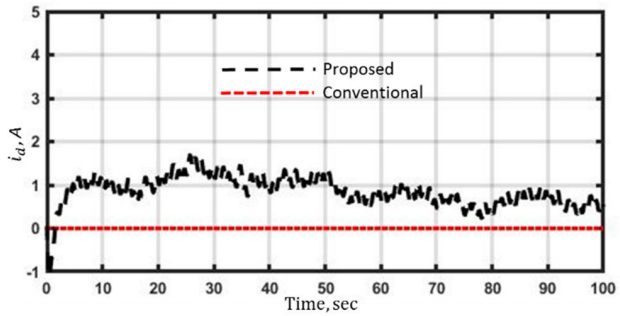


**FIGURE 8.** The presented control and conventional LQR direct current response (scenario 1).

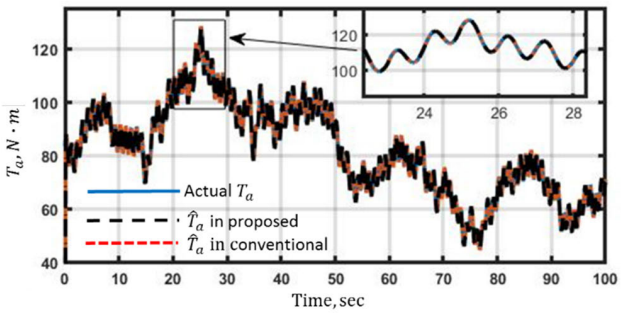


**FIGURE 9.** The presented control and conventional LQR aerodynamic torque estimation with HODO (scenario 1).

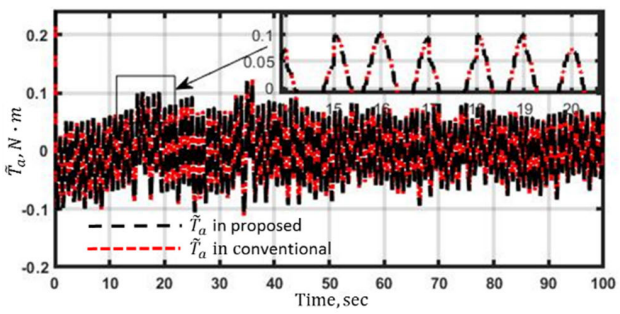


**FIGURE 10.** The presented control and conventional LQR aerodynamic torque estimation errors (scenario 1).

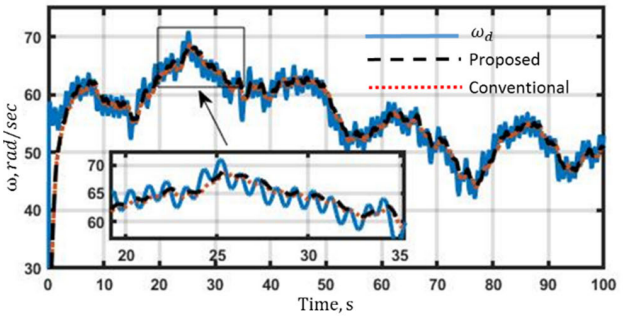


**FIGURE 11.** The presented control and conventional LQR angular shaft speed tracking (scenario 2) [32]. Copyright permission provided.

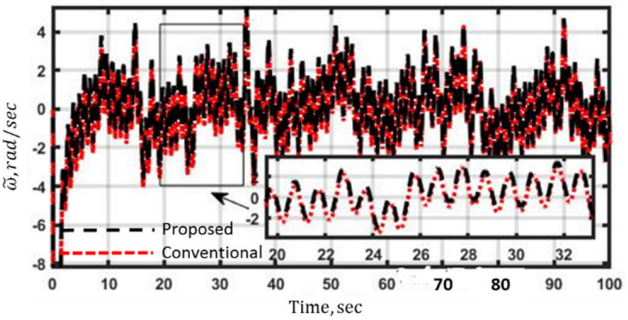


**FIGURE 12.** The presented control and conventional LQR angular shaft speed tracking errors (scenario 2).

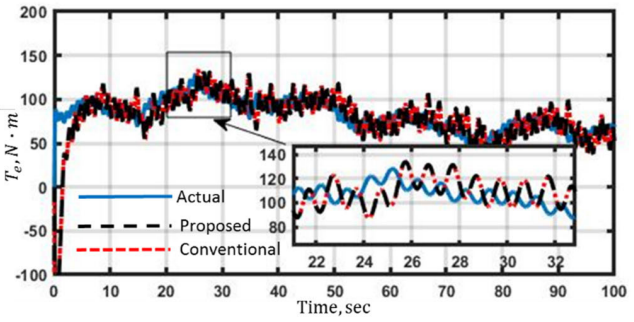


**FIGURE 13.** The presented control and conventional LQR electromagnetic torque tracking (scenario 2) [32]. Copyright permission provided.

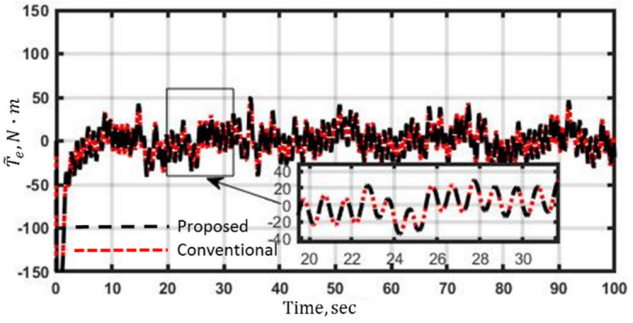


**FIGURE 14.** The presented control and conventional LQR electromagnetic torque errors (scenario 2).

respectively. This might be the effect of the overall reduction of the PMSG's angular shaft speed tracking errors. However, the MAPE of electromagnetic torque $|\tilde{T}_e|$ is slightly increased by 0.3% and 0.45% in both scenarios respectively. Similarly,

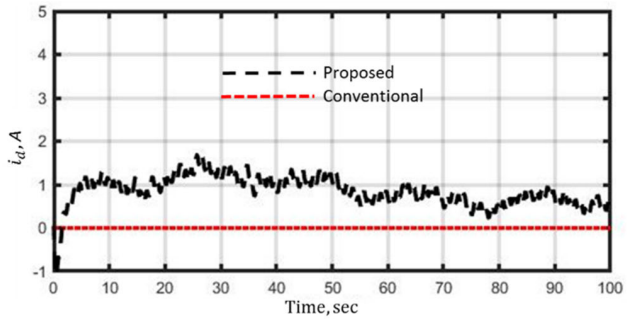


**FIGURE 15.** The presented control and conventional LQR direct current response (scenario 2).

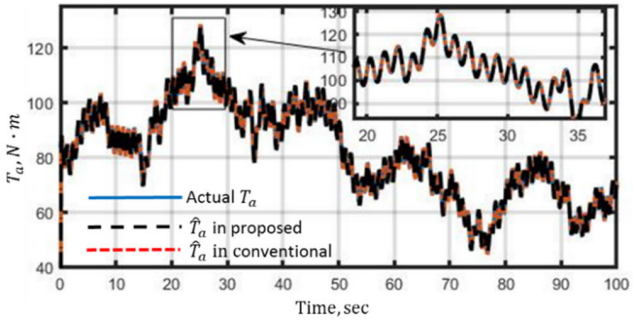


**FIGURE 16.** The presented control and conventional LQR aerodynamic torque estimation with HODO (scenario 2).

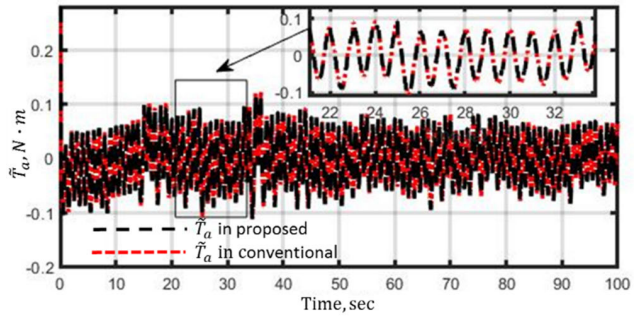


**FIGURE 17.** The presented control and conventional LQR aerodynamic torque estimation errors (scenario 2).

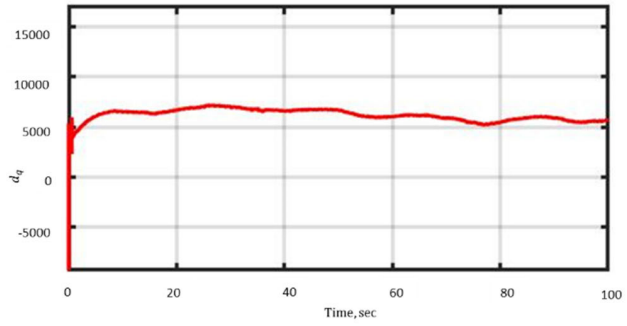


**FIGURE 18.** The quantified disturbance in the quadrature axis (scenario 2) [28]. Copyright permission provided.

the MAE of the direct axis current $\left|\tilde{i}_d\right|$ is slightly more than 0.85 A under the proposed control whereas it is more than

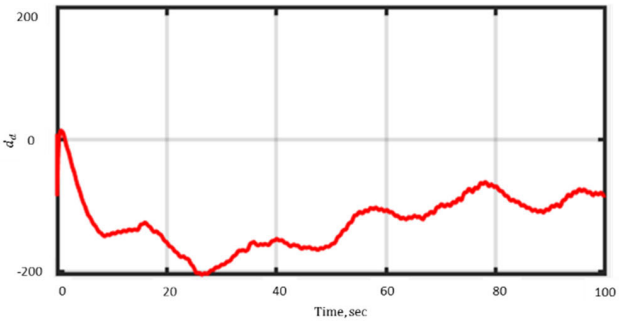


**FIGURE 19.** The quantified disturbance in the direct axis (scenario 2) [28]. Copyright permission provided.

$4.92\times10^{-5}$ A under conventional control algorithm. This might be the result because of the high tunning gain for $T_e$ which was chosen as 1000 (Table 1). Choosing higher gains for $T_e$ and $i_d$ reduces the tracking accuracy of the angular shaft speed of the PMSG.

## IV. CONCLUSION

The servomechanism-based linear feedback controller with LQR for the generator-side power converter is proposed to maximize power extraction of the direct-driven variable-speed WECS. To improve its performance the servomechanism technique is adopted and acts as a penalty state to reduce the angular shaft tracking error. The conventional state-space model was extended with the integral of the generator angular shaft speed error. The tuning gains of extended performance matrices are chosen to obtain satisfactory tracking performance not only under nominal parameters but also under model uncertainty and noise presented scenario. The positive-definite solutions of extended ARE have been obtained offline. Particularly, the MAPE of angular shaft tracking reduced significantly, and the MAPE of electromagnetic torque and MAE of direct axis current slightly increased in both scenarios. The presented control technique demonstrates superior performance over the HODOs-based conventional LQR with the feedforward compensation technique. The HODO has been solely utilized to estimate the aerodynamic torque to adjust the reference angular shaft speed to the wind speed in the WECS application. The closed-loop stability of the presented control technique synthesized with HODO has been proven. The experimental validation of the proposed control is going to be next step to validate the proposed control scheme in the WECS applications.

## ACKNOWLEDGMENT

Nurkhat Zhakiyev and Korhan Kayisli would like to thank Ilhami Colak for the insightful feedback.

## REFERENCES

[1] J. Yang, W.-H. Chen, S. Li, L. Guo, and Y. Yan, "Disturbance/uncertainty estimation and attenuation techniques in PMSM drives—A survey," *IEEE Trans. Ind. Electron.*, vol. 64, no. 4, pp. 3273–3285, Apr. 2017.

[2] S. Das and B. Subudhi, "A robust active and reactive power control scheme with multiloop disturbance rejection for a wind energy conversion system," *IEEE Trans. Sustain. Energy*, vol. 10, no. 4, pp. 1664–1671, Oct. 2019.

[3] T. Ishikawa, N. Igarashi, and N. Kurita, "Failure diagnosis for demagnetization in interior permanent magnet synchronous motors," *Int. J. Rotating Machinery*, vol. 2017, pp. 1–13, Jan. 2017, doi: 10.1155/2017/2716814.

[4] İ. Yazıcı, E. K. Yaylacı, and F. Yalçın, "Modified golden section search based MPPT algorithm for the WECS," *Eng. Sci. Technol., Int. J.*, vol. 24, no. 5, pp. 1123–1133, Oct. 2021, doi: 10.1016/j.jestch.2021.02.006.

[5] A. Fathy, A. G. Alharbi, S. Alshammari, and H. M. Hasanien, "Archimedes optimization algorithm based maximum power point tracker for wind energy generation system," *Ain Shams Eng. J.*, vol. 13, no. 2, Mar. 2022, Art. no. 101548, doi: 10.1016/j.asej.2021.06.032.

[6] E. H. Dursun, H. Koyuncu, and A. A. Kulaksiz, "A novel unified maximum power extraction framework for PMSG based WECS using chaotic particle swarm optimization derivatives," *Eng. Sci. Technol., Int. J.*, vol. 24, no. 1, pp. 158–170, Feb. 2021, doi: 10.1016/j.jestch.2020.05.005.

[7] H. H. H. Mousa, A.-R. Youssef, and E. E. M. Mohamed, "Optimal power extraction control schemes for five-phase PMSG based wind generation systems," *Eng. Sci. Technol., Int. J.*, vol. 23, no. 1, pp. 144–155, Feb. 2020, doi: 10.1016/j.jestch.2019.04.004.

[8] E. Gauterin, P. Kammerer, M. Kühn, and H. Schulte, "Effective wind speed estimation: Comparison between Kalman filter and Takagi–Sugeno observer techniques," *ISA Trans.*, vol. 62, pp. 60–72, May 2016, doi: 10.1016/j.isatra.2015.11.016.

[9] U. H. Khan, Q. Khan, L. Khan, W. Alam, N. Ali, I. Khan, K. S. Nisar, and R. A. Khan, "MPPT control paradigms for PMSG-WECS: A synergistic control strategy with gain-scheduled sliding mode observer," *IEEE Access*, vol. 9, pp. 139876–139887, 2021, doi: 10.1109/ACCESS.2021.3119213.

[10] B. Sarsembayev, K. Suleimenov, B. Mirzagalikova, and T. D. Do, "SDRE-based integral sliding mode control for wind energy conversion systems," *IEEE Access*, vol. 8, pp. 51100–51113, 2020, doi: 10.1109/ACCESS.2020.2980239.

[11] K. Suleimenov, B. Sarsembayev, B. D. H. Phuc, and T. D. Do, "Disturbance observer-based integral sliding mode control for wind energy conversion systems," *Wind Energy*, vol. 23, no. 4, pp. 1026–1047, Apr. 2020, doi: 10.1002/we.2471.

[12] A. V. Le and T. D. Do, "High-order observers-based LQ control scheme for wind speed and uncertainties estimation in WECSs," *Optim. Control Appl. Methods*, vol. 39, no. 5, pp. 1818–1832, Sep. 2018, doi: 10.1002/oca.2444.

[13] T. D. Do, "Disturbance observer-based fuzzy SMC of WECSs without wind speed measurement," *IEEE Access*, vol. 5, pp. 147–155, 2017, doi: 10.1109/ACCESS.2016.2633271.

[14] S. Das and B. Subudhi, "A two-degree-of-freedom internal model-based active disturbance rejection controller for a wind energy conversion system," *IEEE J. Emerg. Sel. Topics Power Electron.*, vol. 8, no. 3, pp. 2664–2671, Sep. 2020, doi: 10.1109/JESTPE.2019.2905880.

[15] S. Li, K. Zhang, J. Li, and C. Liu, "On the rejection of internal and external disturbances in a wind energy conversion system with direct-driven PMSG," *ISA Trans.*, vol. 61, pp. 95–103, Mar. 2016, doi: 10.1016/j.isatra.2015.12.014.

[16] Y. Ma, L. Tao, X. Zhou, and X. Shi, "Analysis and control of fault ride-through capability improvement for wind energy conversion system using linear active disturbance rejection control with correction link," *IEEE Access*, vol. 8, pp. 73816–73827, 2020, doi: 10.1109/ACCESS.2020.2987103.

[17] L. Pan and C. Shao, "Wind energy conversion systems analysis of PMSG on offshore wind turbine using improved SMC and extended state observer," *Renew. Energy*, vol. 161, pp. 149–161, Dec. 2020, doi: 10.1016/j.renene.2020.06.057.

[18] V. Vu and T. D. Do, "A novel nonlinear observer-based LQ control system design for wind energy conversion systems with single measurement," *Wind Energy*, vol. 22, no. 8, pp. 1134–1147, Aug. 2019, doi: 10.1002/we.2345.

[19] V.-P. Vu and T. D. Do, "Observer-based LQR for wind energy conversion systems with single measurement," in *Proc. 4th Int. Conf. Green Technol. Sustain. Develop. (GTSD)*, Nov. 2018, pp. 77–81, doi: 10.1109/GTSD.2018.8595673.

[20] D. Zholtayev, M. Rubagotti, and T. D. Do, "Adaptive super-twisting sliding mode control for maximum power point tracking of PMSG-based wind energy conversion systems," *Renew. Energy*, vol. 183, pp. 877–889, Jan. 2022, doi: 10.1016/j.renene.2021.11.055.

[21] S. Li, M. Cao, J. Li, J. Cao, and Z. Lin, "Sensorless-based active disturbance rejection control for a wind energy conversion system with permanent magnet synchronous generator," *IEEE Access*, vol. 7, pp. 122663–122674, 2019, doi: 10.1109/ACCESS.2019.2938199.

[22] M. Maaruf, M. Shafiullah, A. T. Al-Awami, and F. S. Al-Ismail, "Adaptive nonsingular fast terminal sliding mode control for maximum power point tracking of a WECS-PMSG," *Sustainability*, vol. 13, no. 23, p. 13427, Dec. 2021, doi: 10.3390/su132313427.

[23] B. Majout, B. Bossoufi, M. Bouderbala, M. Masud, J. F. Al-Amri, M. Taoussi, M. E. Mahfoud, S. Motahhir, and M. Karim, "Improvement of PMSG-based wind energy conversion system using developed sliding mode control," *Energies*, vol. 15, no. 5, p. 1625, Feb. 2022, doi: 10.3390/en15051625.

[24] E. H. Dursun and A. A. Kulaksiz, "Second-order sliding mode voltage-regulator for improving MPPT efficiency of PMSG-based WECS," *Int. J. Electr. Power Energy Syst.*, vol. 121, Oct. 2020, Art. no. 106149, doi: 10.1016/j.ijepes.2020.106149.

[25] C. Wei, Z. Zhang, W. Qiao, and L. Qu, "An adaptive network-based reinforcement learning method for MPPT control of PMSG wind energy conversion systems," *IEEE Trans. Power Electron.*, vol. 31, no. 11, pp. 7837–7848, Nov. 2016, doi: 10.1109/TPEL.2016.2514370.

[26] C. Wei, Z. Zhang, W. Qiao, and L. Qu, "Reinforcement-learning-based intelligent maximum power point tracking control for wind energy conversion systems," *IEEE Trans. Ind. Electron.*, vol. 62, no. 10, pp. 6360–6370, Oct. 2015, doi: 10.1109/TIE.2015.2420792.

[27] D. Stansbery and J. Cloutier, "Nonlinear, hybrid bank-to-turn/skid-to-turn missile autopilot design," in *Proc. AIAA Guid., Navigat., Control Conf. Exhib.*, Aug. 2001, pp. 1–10, doi: 10.2514/6.2001-4158.

[28] B. Sarsembayev, D. Zholtayev, and T. D. Do, "Maximum power tracking of variable-speed wind energy conversion systems based on a near-optimal servomechanism control system," *Optim. Control Appl. Methods*, vol. 43, no. 3, pp. 904–924, May 2022, doi: 10.1002/oca.2863.

[29] R. Errouissi, A. Al-Durra, and M. Debouza, "A novel design of PI current controller for PMSG-based wind turbine considering transient performance specifications and control saturation," *IEEE Trans. Ind. Electron.*, vol. 65, no. 11, pp. 8624–8634, Nov. 2018, doi: 10.1109/TIE.2018.2814007.

[30] A. A. Salem, N. A. N. Aldin, A. M. Azmy, and W. S. E. Abdellatif, "A fuzzy logic-based MPPT technique for PMSG wind generation system," *Int. J. Renew. Energy Res.*, vol. 9, no. 4, pp. 1751–1760, 2019, doi: 10.20508/ijrer.v9i4.10138.g7778.

[31] L. Xiaoquan, L. Heyun, and H. Junlin, "Load disturbance observer-based control method for sensorless PMSM drive," *IET Electr. Power Appl.*, vol. 10, no. 8, pp. 735–743, Sep. 2016, doi: 10.1049/iet-epa.2015.0550.

[32] B. Sarsembayev, N. Zhakiyev, A. Akhmetbayev, and K. Kayisli, "Servomechanism based optimal control system design for maximum power extraction from WECS with PMSG," in *Proc. 10th Int. Conf. Smart Grid (icSmartGrid)*, Jun. 2022, pp. 309–313, doi: 10.1109/icSmartGrid55722.2022.9848769.

**BAYANDY SARSEMBAYEV** received the Ph.D. degree in technical sciences in transport operation from the Kazakh Academy of Transport and Communications, Almaty, Kazakhstan, in 2005, the M.Sc. degree in systems and control engineering from the City University of London, London, U.K., in 2015, and the Ph.D. degree in electrical engineering and electronics research from Brunel University London, U.K., in February 2023. Also, he has industrial experience with Kazakhstan National Railway Company, as a Railway Worker in Station Control System and Safety Specialist, in 2000 and 2008, respectively. From 2001 to 2007, he was with the Transport Studies Department, Kazakh Academy of Transport and Communications, as an Instructor. From 2008 to 2012, he was with the Transport Studies Department, L. N. Gumilyov Eurasian National University, Astana, Kazakhstan, as an Instructor. Since July 2017, he has been a Research Assistant with the School of Engineering and Digital Sciences, Nazarbayev University, Kazakhstan, for several funded projects. His research interests include the design of advanced control techniques to improve the performance of permanent magnet synchronous machine applications, LiPo battery modeling in dynamic wireless power transfer for UAV applications, high-performance triboelectric nanogenerators designed for mechanical energy harvesting, and self-powered tactile sensor applications.

**NURKHAT ZHAKIYEV** received the Ph.D. degree in physics from Eurasian National University, Kazakhstan, in 2015. Since 2020, he has been a Senior Researcher and the Director of the Department of Science and Innovation, Astana IT University, Kazakhstan. He was a supervisor of several research projects on the energy system modeling and integration of renewables. He was a Computer Modeler in energy systems and a Climate Change Mitigation Expert with UNDP. From March 2022 to March 2023, he was a Postdoctoral Researcher with the Engineering Faculty, Gazi University, Ankara, Turkey. He is the author of several articles published in international journals and a reviewer of many ISI journals.

**ALMAN KUSHEKKALIYEV** received the Ph.D. degree in physics and mathematical science, in 2004. Currently, he is an Associate Professor with the Department of Physics, West Kazakhstan University. He is the author of several articles published in peer-reviewed journals and conferences. His research interests include the design of advanced control systems and modeling in physics of mechanical energy.

**KORHAN KAYISLI** (Senior Member, IEEE) received the B.Sc. degree in electronics education from Sakarya University, Turkey, in 2001, and the M.Sc. and Ph.D. degree in electronics and computer science from Firat University, Turkey, in 2004 and 2012, respectively. Between 2002 and 2012, he was a Research Assistant with Firat University, Bitlis Eren University, Gelisim University, and Nisantasi University, respectively. Additionally, he was a Researcher in two EU mobility projects. He is currently an Associate Professor with the Department of Electrical and Electronics Engineering, Engineering Faculty, Gazi University, Ankara, Turkey. His research interests include renewable energy, intelligent systems, power electronics, converter circuits, power factor correction, robust control, and educational technologies. He is a Co-Editor of the *International Journal of Renewable Energy Research* and *International Journal of Engineering Science and Application* and an Editor of the *Electric Power Components and Systems* journal. He also served as a reviewer of peer-reviewed journals.

**TON DUC DO** (Senior Member, IEEE) received the B.S. and M.S. degrees in electrical engineering from the Hanoi University of Science and Technology, Hanoi, Vietnam, in 2007 and 2009, respectively, and the Ph.D. degree in electrical engineering from Dongguk University, Seoul, South Korea, in 2014. From 2008 to 2009, he was with the Division of Electrical Engineering, Thuy Loi University, Vietnam, as a Lecturer. He was with the Division of Electronics and Electrical Engineering, Dongguk University, as a Postdoctoral Researcher, in 2014. He was also a Senior Researcher with the Pioneer Research Center for Controlling Dementia by Converging Technology, Gyeongsang National University, South Korea, from May 2014 to August 2015. Since September 2015, he has been an Assistant Professor and then an Associate Professor with the Department of Robotics and Mechatronics, Nazarbayev University, Kazakhstan. His research interests include advanced control system theories, electric machine drives, renewable energy conversion systems, and nanorobots. He received the Best Research Award from Dongguk University, in 2014, the Most Cited Paper Award from Wind Energy, in 2020 and 2021, and the Outstanding Associate Editor of IEEE Access, in 2021. He was recently listed in the top 2% of the most influenced scientists in the world, in November 2022. He has been an Associate Editor of IEEE Access, since April 2017. He has been also a Guest Editor for special issues of several journals, such as *Mathematical Problems in Engineering*, *Electronics*, *Energies*, and *Sensors*.